Distribution of Variances of Single Molecules in a Disordered Lattice

E. Barkai and R. Silbey*

Department of Chemistry and Center for Material Science and Engineering, Massachusetts Institute of Technology, Cambridge, Massachusetts 02139

Received: July 20, 1999; In Final Form: October 26, 1999

Single molecule spectroscopy in disordered lattice is investigated from a theoretical point of view. We consider energy fluctuations of the molecule due to dipolar interactions with two level system (TLS) defects distributed randomly on a three-dimensional cubic lattice. Each independent TLS is randomly flipping so the energy of the molecule is time dependent. We investigate the probability distribution $g(W)$ of the variance of the energy fluctuations. The exact solution, found for finite systems, exhibits peaks, peaks within peaks, etc., corresponding to interaction with nearest neighbors, next-nearest neighbors, etc. For an infinite crystal at high defect density, the distribution of W is shown to depend strongly on the interaction with nearest neighbors and hence on lattice symmetry. At low defect density, $g(W)$ exhibits several peaks separated by large gaps in which $g(W) \sim 0$. We explain these peaks in terms of contributions from single defects located on discrete distances from the molecule. For the continuum version of our model, $g(W)$ is a Lévy stable nonsymmetrical probability density function, decaying according to $g(W) \sim W^{-3/2}$. We discuss the relation between the continuum and lattice models.

I. Introduction

Modern experimental techniques have made it possible to perform time dependent measurements of the optical spectrum of a single molecule embedded in a solid. Using single-molecule spectroscopy (SMS), one may study many spectroscopic details obscured by inhomogeneous line broadening[1] observed when the line shape of an ensemble of molecules is investigated.[2−6]

When single-molecule spectra are measured in disordered solid, one sees that molecules are in a unique environment that fluctuates in time, thus giving rise to a variety of time dependent phenomena. The transition energy $E(t)$ of each molecule is time dependent and since each molecule is unique, the random process $E(t)$ varies from one molecule to the other. We assume here that each molecule can be characterized by a variance $W = \overline{(E(t)-\overline{E(t)})^2}$ where the bar denotes time averaging or standard thermal equilibrium averaging. Depending on its environment, W will vary from one molecule to the other. Our aim in this paper is to calculate the distribution of W using a simple model.

At least in principle the variance W could be measured based upon single molecule spectroscopy. For example, single-molecule spectroscopy of pentacene in *p*-terphenyl (disordered) crystals, at low temperatures, reveals two classes of molecules.[7] The first have time independent resonant frequencies while the second exhibits a random walk in frequency space. Various types of such spectral diffusions are observed the typical jump length varying from one molecule to the other. Since the spectral diffusion is clearly bounded by the inhomogeneous line width and assuming equilibrium is reached on the time scale of the experiment, such a spectral random walk is characterized by a finite variance W.

We consider a cubic lattice model with the single chromophore at the origin and with each lattice point having a probability p being occupied by a two level system (TLS). In this way we study different single molecule spectrum with each configuration of TLSs. Each TLS is flipping, leading to a time dependent transition energy for the chromophore. We neglect the interaction among the TLSs and consider only the interaction between the TLSs and chromophore. Similar, but distinct, models have been used to understand the thermal properties and the time dependence of various spectroscopic experiments, such as hole burning, photon echo decay, as well as single molecule spectra.[8−20]

We calculate the probability density function of the variance of the transition energy fluctuations $g(W)$. We show that the lattice structure has a strong influence on $g(W)$. We first consider the case $p = 0.5$, i.e., strong disorder, in detail, and calculate the distribution of variance exactly for finite systems. For infinite system the solution is shown to reflect the lattice symmetry, exhibiting seven distinct Gaussian peaks corresponding to six nearest neighbors. We then consider the case of p small, i.e., weak disorder, and compare the lattice results to earlier continuum results.

A brief report of our study was presented in ref 21. The present paper is organized as follows. In section II, the lattice model is stated, and we elaborate on the relation between the distribution of variances and distribution of line widths that has been measured in several disordered materials. Then in section III we find the exact solution of our model. In section IV we present the exact solution for finite systems and discuss its degeneracy. In section V we find an approximate solution for the infinite system and for strong disorder $p = 1/2$, which helps us to clarify the meaning of the exact results. In section VI we analyze the continuum version of the model using the fundamental generalized central limit theorem.[22−24] The weak disorder case is investigated in section VII. We give an approximate solution valid for weak disorder and compare between the continuum and lattice models. Finally a discussion of our results as well as other related results is given in section VIII.

* Corresponding author. Fax: +1-617-253-7030. E-mail: silbey@mit.edu.

10.1021/jp9924880 CCC: $19.00
Published on Web 12/22/1999

II. Lattice Model

Consider a single molecule (e.g., a chromophore) interacting with defect dipoles which are randomly distributed in space. The molecule resides on the origin of a three-dimensional cubic lattice. The lattice spacing is a. Each site is labeled with an index j. Site j (not including the origin) is described with an occupation parameter β_j, which can take the values 0 or 1, corresponding to the absence and presence of a defect that flips on the time scale of the experiment. The probability that lattice site j is occupied is p. We assume that the occupancy of site j is independent of the occupancy of other lattice sites.

Let us assume that the defects are uncorrelated TLSs interacting with a chromophore by a dipolar interaction. The TLS chromophore interaction was analyzed in[9,10,16] within the stochastic sudden jump approach which considers a continuum medium. Within this model every flip of a two level system is assumed to shift the transition energy of the chromophore by the amount $E_j = 2\alpha\epsilon_j/|\vec{r}_j|^3$. α is a coupling constant, and $\vec{r}_j$ is the position of the defect on site j. ϵ_j are time independent orientation parameters, taken to be $+1$ or -1 with equal probability. The total energy of the chromophore is a sum of contributions from different defects

$$E(t) = \sum_j \alpha \frac{\beta_j \epsilon_j \xi_j(t)}{|\vec{r}_j|^3} \tag{2.1}$$

where the sum is over all lattice points excluding the origin. $\xi_j(t)$ is a time dependent occupation parameter taken to be 1 or 0, corresponding to the jth TLS being in its ground or excited state, respectively. We assume that all stochastic processes are independent and statistically identical. That is, we assume that we can treat the defects as either flipping rapidly on the time scale of the experiment or frozen on that time. The time average $\overline{(\xi_i(t)-\bar{\xi}_i(t))^2} \equiv \delta^2$ is given by standard thermal equilibrium occupation of the ground and first excited states of the identical TLSs.

According to the model's assumption, we have

$$\overline{E(t)} = \alpha\bar{\xi}\sum_j \frac{\epsilon_j\beta_j}{|r_j|^3} \tag{2.2}$$

We define the dimensionless distance $|j|$ with $|\vec{r}_j| \equiv a|j|$, and hence the variance of the energy fluctuations is given by

$$W \equiv \frac{a^6(\overline{E^2} - \bar{E}^2)}{\delta^2\alpha^2} = \sum_j \frac{\beta_j}{|j|^6} \tag{2.3}$$

W in eq 2.3 will vary from one molecule to the other depending on the environment each is situated in. In this paper we investigate the statistical properties of the dimensionless random variable W.

Under certain conditions the variance W is related to a line width $\delta\nu$.[8,9] Experiments[8,25−27] in glassy and defected crystalline materials have shown that different guest molecules have different line widths (the stable line shapes were all very much the same). These experiment found that $h(\Delta\nu)$, the probability density of line widths of single molecules, is asymmetrical and long tailed. The line width $\Delta\nu$ was related to the variance W according to

$$\Delta\nu = z\sqrt{W} \tag{2.4}$$

and the dimensionless factor z depends on the line shape.[9] Such a relation between line width and variance is possible only when the line shape has a simple shape (e.g., a Gaussian); if the line shapes split due to strong coupling with defects or if the variance of line shape diverges (e.g., Lorentzian line shape), clearly relation eq 2.4 does not hold. Using eq 2.4 the probability density of line widths $h(\Delta\nu)$ is related to the probability density of variances according to

$$h(\Delta\nu) = (2\Delta\nu/z)\, g\,[(\Delta\nu)^2/z^2] \tag{2.5}$$

To analyze the experimental data in noncrystalline media, a continuum model was analyzed[8,9,28] [i.e., the continuum version of eq 2.3]. Currently, there is not sufficient experimental data to determine whether the continuum theory works quantitatively.

III. The Distribution of the Variance: Exact Results

A. Tools and Definitions. Our aim in this section is to investigate the probability, Prob $(W = x)$, of finding a variance W equal to x. This probability function can be formally found for any finite system. For finite systems, Prob $(W = x) \neq 0$ only on a finite number of points x.

One may limit the investigation of the model to $0 < p \leq {}^1/_2$. For $p > {}^1/_2$, one can redefine the problem where vacancies (i.e., empty lattice points) are considered as defects. One can show that

$$\mathrm{Prob}_q\left(W = \frac{1}{2}I(1) + x\right) = \mathrm{Prob}_{-q}\left(W = \frac{1}{2}I(1) - x\right) \tag{3.1}$$

where $q \neq p - {}^1/_2$ is a control parameter and $I(1) \equiv \sum_j 1/|j|^6$.

The variance W, eq 2.3, is bounded by $0 < W \leq I(1)$. This implies that all moments of Prob $(W = x)$ converge. The first two moments of the variance W are given by

$$\langle W\rangle = pI(1)$$

$$\langle W^2\rangle = \langle W\rangle^2 + p(1-p)\, I\,(2) \tag{3.2}$$

with

$$I(n) \equiv \sum_j \frac{1}{|j|^{6n}} \tag{3.3}$$

where $n = 1, 2, \ldots$. The averaging $\langle\ldots\rangle$, in eq 3.2, is over the occupation parameters $\{\beta_j\}$. The converging sums $I(n)$ are evaluated using a computer, without difficulty. They can also be evaluated using standard continuum approximation which replaces the summation in eq 3.3 with an integration.[29] In Table 1 we give the numerical values of $I(n)$, and we see that $\lim_{n\to\infty} I(n) = 6$ which is the number of nearest neighbors on a cubic lattice.

Let $n_{|j|^2}^{\max}$ be the number of sites on the cubic lattice that are a distance $|j|^2 = 1, 2, 3, \ldots$ from the origin. For example,

$$n_1^{\max} = 6,\ n_2^{\max} = 12,\ n_3^{\max} = 8,\ n_4^{\max} = 6,\ n_5^{\max} = 24$$

$$n_6^{\max} = 24,\ n_7^{\max} = 0,\ n_8^{\max} = 12$$

$$n_9^{\max} = 30,\ n_{10}^{\max} = 24,\ n_{11}^{\max} = 24$$

and from a standard continuum approximation $n_{|j|^2}^{\max} \sim 2\pi|j|$ for $|j| \gg 1$. We do not know of an explicit formula for $n_{|j|^2}^{\max}$; however, these numbers can be easily calculated for large systems.

TABLE 1

n	1	2	3	4	5	6
$I(n)$	8.401 84	6.202 15	6.023 88	6.002 95	6.000 37	6.000 05

A disordered system is characterized by n_1 TLSs a distance $|j|^2 = 1$ from the origin, n_2 TLSs a distance $|j|^2 = 2$, etc. We define a disordered state with the sequence of numbers $\{n_1, n_2, ..., n_m\}$. m is an upper cutoff which gives the number of "shells" we consider.

B. Exact Solution. To find the exact solution we use the characteristic function defined in Fourier k space,

$$\langle \exp(ikW) \rangle = \prod_j [p \exp(ik/|j|^6) + (1 - p)] \qquad (3.4)$$

The product $\prod_j$ is over all lattice points. As we show in the Appendix, one can use the lattice symmetry and the characteristic function to obtain the solution for finite systems

$$\text{Prob}(W = x) = \sum_{n_1,n_2,...,n_m|x} \binom{n_1^{\max}}{n_1}\binom{n_2^{\max}}{n_2}...\binom{n_m^{\max}}{n_m} \times p^{\sum_{i=1}^m n_i}(1 - p)^{N - \sum_{i=1}^m n_i} \qquad (3.5)$$

where $N = \sum_{i=1}^m n_i^{\max}$ is the number of lattice sites. In eq 3.5 $\sum_{n_1,n_2,...n_m|x}$ is a sum over all values of

$$n_1 = 0, ..., n_1^{\max}$$

$$\vdots$$

$$n_m = 0, ..., n_m^{\max} \qquad (3.6)$$

which satisfy the condition

$$x = n_1 + n_2/2^3 + ... n_m/m^3 \qquad (3.7)$$

For $x \neq n_1 + n_2/2^3 + ... n_m/m^3$ we have Prob $(W = x) = 0$.

Eq 3.7 describes the discrete variance spectrum.

To calculate Prob $(W = x)$, given in eq 3.5, for all values of x for which Prob $(W = x) \neq 0$ we have to consider

$$g_m = (n_1^{\max} + 1)(n_2^{\max} + 1)...(n_m^{\max} + 1) \qquad (3.8)$$

disordered states. This is much smaller than a straightforward consideration of all

$$c_m = (2)^{\sum_{q=1}^m n_q^{\max}} \qquad (3.9)$$

microscopic configurations. Our method uses the symmetry of the lattice and the fact that the TLSs which are a distance $|j|$ from the molecule contribute in the same way to the characteristic function helped us reduce the number of configurations we must consider. For a three-dimensional system we have $g_{11} \simeq 2^{39.7} \ll c_{11} = 2^{170}$ and $g_5 \simeq 2^{17.1} \ll c_5 = 2.^{54}$

IV. Strong Disorder $p = 1/2$

For the case $p = 1/2$, the disorder is strong and the contribution to Prob $(W = x)$ from nearest neighbor interaction is nonnegligible. In this case we may expect the lattice structure to play an important role controlling the shape of Prob $(W = x)$.

To generate the solution we begin with a system with only nearest neighbors interaction. In Figure 1a we show Prob $(W = x)$ for the three-dimensional cubic lattice and $p = 1/2$. There are seven peaks in the figure corresponding to seven states in which the system can be found these being an empty system, a system with one occupied site, etc. In Figure 1b we consider a larger system including the next nearest neighbors interaction. We see that each peak has split due to the interaction with the next nearest neighbors. The axis of symmetry of Figure 1a is on $x = 3$. This axis is shifted to $3 + 6/2^3$ in Figure 1b; in the thermodynamic limit of $m \to \infty$, the axis of symmetry is on $I(1)/2$ (see details below).

We have emphasized already that there exists a degeneracy in the model since different microscopic configurations contribute in the same manner to Prob $(W = x)$. This has helped us reduce the number of disordered states needed for the calculation: for nearest and next nearest interaction, this means that we can easily reduce the problem from its $c_2 = 2^{18}$ microscopic configurations to $g_2 = 7 \times 13 = 91$ disordered states. We observe a second type of degeneracy when the interaction with next nearest neighbors are included. In Figure 1b we observe only $61 < g_2 = 91$ values of W for which Prob $(W = x) \neq 0$. To understand this degeneracy consider the two states with $n_1 = 1$, $n_2 = 8$ and $n_1 = 2$, $n_2 = 0$. Since for both cases the value of $W = 1 + 8/2^3 = 2 + 0/2^3 = 2$, we have a second degeneracy in the problem. We call this accidental degeneracy.

For practical reasons one must carry the calculations of the sums in eq 3.5 with the aid of a computer. However, numerical inaccuracy might remove the accidental degeneracy. Hence, to find the exact solution for Prob $(W = x)$, it is important to use exact numerical tools which can identify all the degeneracy in the problem (e.g., we used Mathematica). As we shall later show the accidental degeneracy is a significant ingredient in this problem: its accidental removal alters the shape of Prob $(W = x)$.

In Figures 1c,d we show the solution for even larger systems. A detailed structure is emerging. Notice that as we increase the size of the system the height of the observed peaks is attenuated while the number of peaks increases. As we increase the systems' size, the central peaks are shifting to the right. In Figure 2 we have indicated the location of seven peaks in the limit of an infinite system (see more details below).

It is instructive to rewrite eq 3.5 as a sum of seven terms

$$\text{Prob}(W = x) = \sum_{j_1=0}^{6} Q_{j_1} \text{Prob}(W = x|n_1 = j_1) \qquad (4.1)$$

Where Prob $(W = x|n_1 = j_1)$ is the conditional probability that $W = x$ when the number of occupied nearest neighbors is equal j_1 and

$$Q_{j_1} = p^{j_1}(1 - p)^{6 - j_1}\binom{6}{j_1} \qquad (4.2)$$

is the probability that j_1 nearest neighbors sites are occupied. The conditional probability is given by

$$\text{Prob}(W = x|n_1 = j_1) = \sum_{j_1,n_2,...,n_m|x}{}' \binom{n_2^{\max}}{n_2}...\binom{n_m^{\max}}{n_m} \times p^{\sum_{q=2}^m n_q}(1 - p)^{N - 6 - \sum_{q=2}^m n_q} \qquad (4.3)$$

and the summation procedure is defined in eq 3.5 with $n_1 = j_1$.

In Table 2 we give the cumulant expansion of Prob $(W = x|n_1 = j_1)$ valid in the thermodynamic limit of large

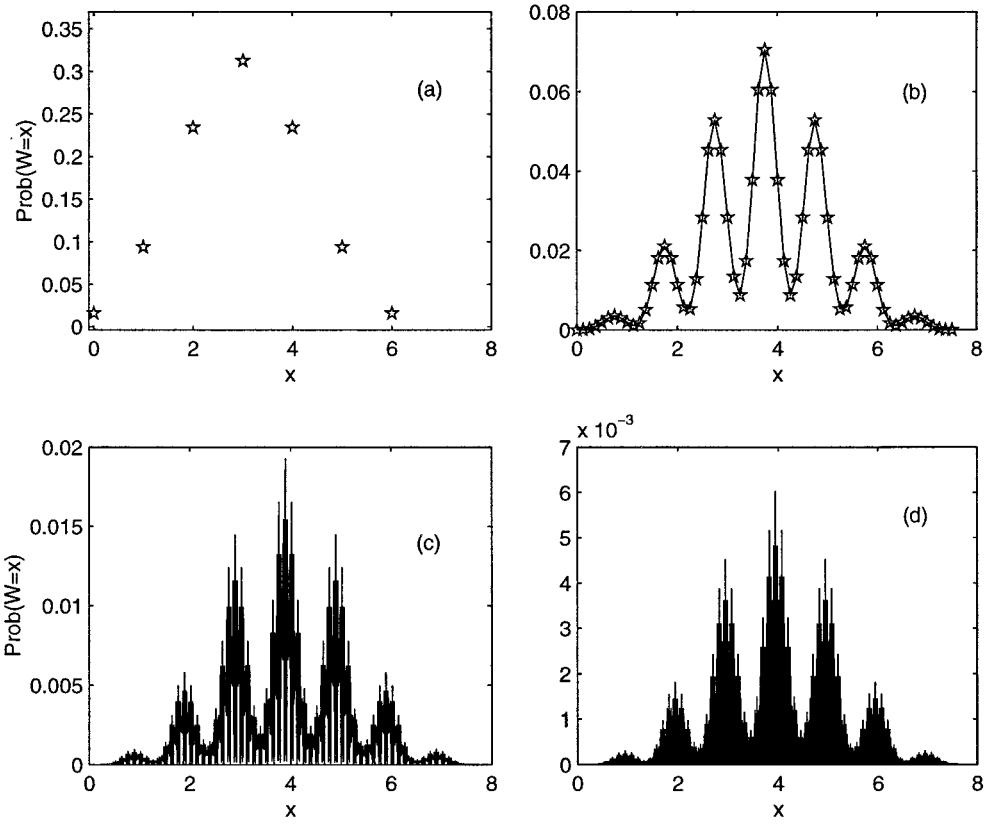

Figure 1. Prob ($W = x$) for $p = {}^1/_2$ and for different system size. (a) Only interaction with the nearest neighbors is considered and then seven delta peaks are observed. (b) We consider the interaction with nearest neighbors and next-nearest neighbors (i.e., $m = 2$). Notice the horizontal shift of the axis of symmetry relative to case (a). The continuous curve is added to guide the eye, and 61 delta peaks are observed. (c) Now $m = 3$, notice the change of scale compared to previous cases; 549 delta peaks are observed. Case (d), now $m = 4$ so the maximum number of TLSs in the system is 32; 3843 delta peaks are observed.

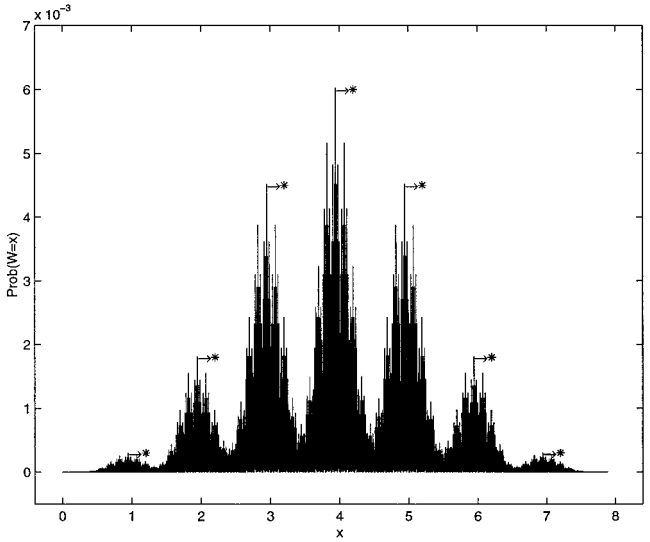

Figure 2. The same as Figure 1d, Prob ($W = x$) with $m = 4$. We have indicated the fixed points (stars), found in eq 4.8 below, to which the peaks of the distribution are converging in the thermodynamic limit. Also shown is the direction of flow (arrows).

system. To find the cumulants κ_n we have used the conditioned characteristic function

$$\langle \exp(ik\cdot W)\rangle_{n_1=j_1} = \mathrm{e}^{ikj_1}\{\prod_{j\neq j_1}[p\exp(ik/|j|^6) + (1-p)]\} \quad (4.4)$$

where $\prod_{j\neq j_1}$ is a multiplication over all lattice points excluding the nearest neighbors, and the standard definition of the

TABLE 2

n	κ_n
1	$j_1 + (1/2 + q)[I(1) - 6]$
2	$(1/4 - q^2)[I(2) - 6]$
3	$-2(1/4 - q^2)q[I(3) - 6]$
4	$(1/4 - q^2)(-1/2 + 6q^2)[I(4) - 6]$
5	$(1/4 - q^2)(4q - 24q^3)[I(5) - 6]$
6	$(1/4 - q^2)(1 - 30q^2 + 120q^4)[I(6) - 6]$
7	$(1/4 - q^2)(-17q + 240q^3 - 720q^5)$ $[I(7) - 6]$
8	$(1/4 - q^2)(-17/4 + 231q^2 - 2100q^4 + 5040q^6)$ $[I(8) - 6]$

cumulant expansion

$$\ln[\langle \exp(ikW)\rangle_{n_1=j_1}] \equiv \sum_{n=1} i^n \frac{\kappa_n}{n!} k^n \quad (4.5)$$

The cumulants in Table 2 are given in terms of $q \equiv p - {}^1/_2$. We have calculated the cumulants using symbolic programming (e.g., we used Mathematica without which the calculation becomes cumbersome).

A few features can be seen in Table 2. First for $p = 1$ or $p = 0$ (i.e., $q = \pm{}^1/_2$) all the cumulants excluding the first are identically zero. This is expected from distributions concentrated on a point. The odd (even) cumulants are odd (even) functions of q. Using this odd/even property it is straightforward to prove eq 3.1. The nth cumulant is proportional to $I(n) - 6$, six being the number of nearest neighbors. As we show in Table 1, the difference $I(n) - 6$ approaches zero exponentially fast when n is increased. For $p = {}^1/_2$ (i.e., $q = 0$) all odd cumulants (excluding the first) of Prob ($W = x|n_1 = j_1$) are identically

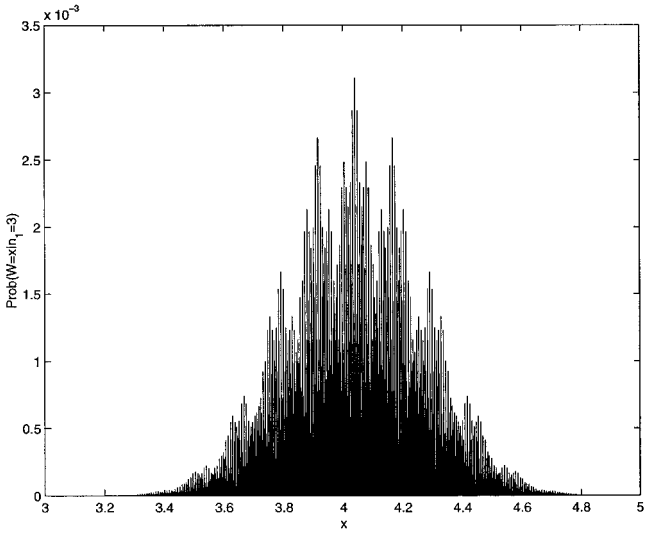

Figure 3. Prob ($W = x|n_1 = 3$) for a system with 56 lattice points (i.e., $m = 5$) and $p = 1/2$. Besides an attenuation factor, and small shift, this structure is very similar to that observed in the central part of Prob ($W = x$) in Figures 1c,d and 2.

zero as expected from a symmetric distribution. Later we shall use the cumulants to find an approximate solution for an infinite lattice system.

The conditioned moments are given by

$$\langle W\rangle_{n_1=j_1} = \kappa_1 = j_1 + p[I(1) - 6] \tag{4.6}$$

and

$$\sigma^2 = \kappa_2 = \langle W^2\rangle_{n_1=j_1} - \langle W\rangle^2_{n_1=j_1} = p(1-p)[I(2) - 6] \tag{4.7}$$

For $p = 1/2$ the axis of symmetry of the seven conditional probabilities is located at $\langle W\rangle_{n_1=j_1}$. We believe, but have no proof, that on these locations the conditional probability attains its maximal value. In the limit of infinite system these points are given by

$$x = I(1)/2, \quad x = I(1)/2 \pm 1, \quad x = I(1)/2 \pm 2 \tag{4.8}$$

These are the points shown in Figure 2. Equation 4.8 implies that the axis of symmetry of Prob ($W = x$) is on $I(1)/2$.

A useful identity is

$$\text{Prob}\,(W = x|n_1 = j_1) = \text{Prob}\,(W = x+1|n_1 = j_1 + 1) \tag{4.9}$$

which can be easily understood from eq 4.3. The identity eq 4.9 is useful for numerical computations. The calculation of Prob ($W = x$) can follow two steps: first calculate Prob ($W = x|n_1 = 0$) and then with eqs 4.1 and 4.9 calculate Prob ($W = x$) for all the spectrum of x. This method further reduces the computation time.

In Figure 3 we show the conditional probability Prob ($W = x|n_1 = 3$) for a system with $m = 5$. Not surprisingly the structure we observe is very similar to the structure of the central part of Prob ($W = x$) shown in Figures 1c,d and 2 for smaller systems [i.e., Prob ($W = x$) for $3.2 < x < 4.8$]. In Figure 4 we show Prob ($W = x|n_1 = 3$) for a larger system with $m = 6$. Now the detailed structure of Prob ($W = x|n_1 = 3$) is very different than that shown in Figure 3. Many new peaks are observed which are not observed in the smaller systems.

The emergence of this new structure is due to the accidental degeneracy we discussed previously. In Figure 4 we have marked two points as D_0 and D_1. We have found the disordered

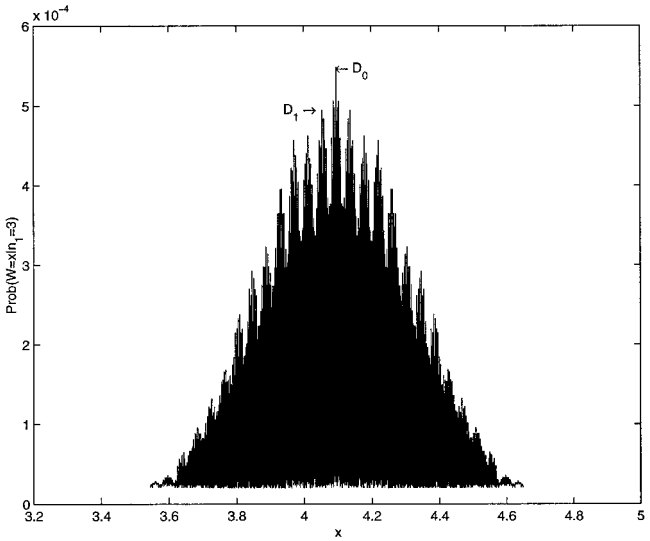

Figure 4. Prob ($W = x|n_1 = 3$) for a system of 80 lattice points (i.e., $m = 6$), $p = 1/2$. Two highly degenerate peaks D_0 and D_1 are discussed in the text. The structure is very different from the structure shown in Figure 3.

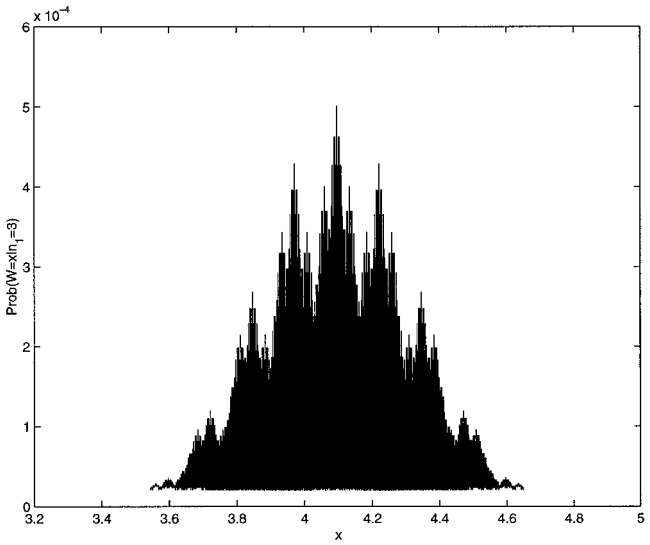

Figure 5. The same as in Figure 4; however, now we have removed the accidental degeneracy. Comparing this figure and Figure 4 we see that the accidental degeneracy gives an important contribution to the fine structure of Prob ($W = x|n_1 = 3$).

states which contribute to these peaks. We have defined a disordered state with the sequence $\{n_1, n_2, ..., n_m\}$ describing n_1 defects a distance $|j|^2 = 1$ from the origin, n_2 defects a distance $|j|^2 = 2$ from the origin, etc., and for our case $m = 6$. Seven disordered states contribute to D_0, these being

$$\{3,5,7,3,12,15\}, \quad \{3,5,8,3,12,7\}, \quad \{3,6,3,3,12,20\}$$

$$\{3,6,4,3,12,12\}, \quad \{3,6,5,3,12,4\}, \quad \{3,7,0,3,12,17\}$$

$$\{3,7,1,3,12,9\}$$

six disordered states contribute to D_1

$$\{3,5,7,3,12,7\}, \quad \{3,5,6,3,12,15\}, \quad \{3,6,2,3,12,20\}$$

$$\{3,6,3,3,12,12\}, \quad \{3,6,4,3,12,4\}, \quad \{3,7,0,3,12,9\}$$

To see that all these disordered states contribute to the same peak one can easily check that x defined in eq 3.7 is identical

for all the listed states. To illustrate the importance of this accidental degeneracy, we show in Figure 5 the conditional probability Prob ($W = x|n_1 = 3$) for the same system as in Figure 4; however, now we artificially remove the degeneracy. Clearly, Figure 4 (degenerate and correct) and Figure 5 (nondegenerate) are nonsimilar. The accidental degeneracy plays an important role in the shape of Prob ($W = x$) for finite systems. It is interesting to remark that the degeneracy of the smaller systems shown in Figures 1−3 is weaker [i.e., the points D_0, D_1 (and many others) are nondegenerate when $m < 6$].

Finally, we emphasize that the degeneracy can be partially or fully removed by different physical mechanisms, which break the lattice symmetry. We believe that this degeneracy implies that the exact solution exhibits a strong sensitivity to perturbations of different types.

V. Distribution of the Variance: Approximate Results

Our exact results presented in Figures 1−5 were obtained for a finite systems. Let us consider a simple approximate solution for an infinite lattice and $p = 1/2$. When $p = 1/2$ the cumulants in Table 2 show $\kappa_{2n+1} = 0$ and

$$3\kappa_2^2 \gg \kappa_4$$

$$15\kappa_2^3 \gg \kappa_6 + 15\kappa_4\kappa_2 \tag{5.1}$$

(e.g., $3\kappa_2^2/\kappa_4 \simeq 21.3$). When these inequalities are satisfied, the conditioned probability $P(W = x|j = n_1)$ behave like the Gaussian distribution (i.e., it is well-known that the cumulants of the Gaussian vanish for $n > 2$). Our approximation neglects all contributions from the conditioned cumulants κ_n in Table 2 with $n > 3$, namely Prob ($W = x|n_1 = j1$) is replaced with a Gaussian with the variance and mean given in eqs 4.6 and 4.7 when $p = 1/2$. Therefore, let $g(W)dW$ be the probability of finding the variance in a small interval (W, $W + dW$), then

$$g(W) = \sum_{j_1=0}^{6} Q_{j1} \frac{1}{\sqrt{2\pi\sigma_1^2}} \exp\left[-\frac{(W - j_1 - \upsilon)^2}{2\sigma_1^2}\right] \tag{5.2}$$

where

$$\sigma_1^2 = \frac{[I(2) - 6]}{4} \tag{5.3}$$

and

$$\upsilon = \frac{[I(1) - 6]}{2} \tag{5.4}$$

In eq 5.2 the sum over j_1 reflects the contribution from the six nearest neighbors interaction while the finite width of the seven Gaussians reflects the interaction with the background. As can be seen in Figure 6 the variance σ_1^2 defined in eq 5.3 is large enough to insure a significant overlap between the nearest neighbors conditional probabilities.

The approximation $g(W)$, in eq 5.2, is a smooth continuous probability density function which replaces the exact expression for $g(W)$, eq 3.5, which is a sum of closely spaced delta function. To compare between the exact and approximate solution we have built a histogram based on the exact solution. This histogram is shown in Figure 6 together with the approximation eq 5.2. The exact result was derived for a finite system, with $m = 8$, for which the exact solution has not yet reached its thermodynamic ($m \to \infty$) limit. To overcome this obstacle we used also eq 4.8, which gives the exact location of the axis of symmetry of the seven conditional probabilities. Hence, we shift (slightly) the exact finite size solution, in such a way that the axis of symmetry of $g(W)$ is on $I(1)/2$. This is how we obtain good agreement between exact and approximate solution.

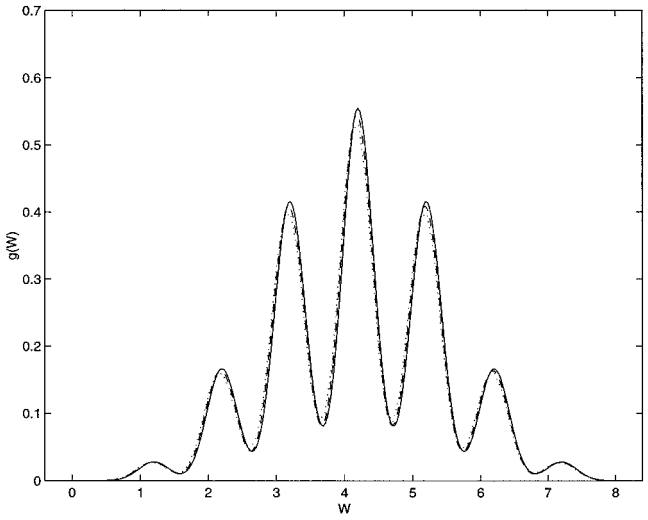

Figure 6. The solid curve is $g(W)$, eq 5.2, exhibiting seven peaks which are due to the lattice symmetry. The dotted curve is a histogram (with a bin length 0.1) obtained with the exact result for a finite system with $m = 8$. Also shown (dashed curve) is the solution obtained by a numerical Fourier inversion of the characteristic function eq 3.4. Good agreement between the exact, approximate and numerical results is obtained.

TABLE 3

n	κ_n exact	κ_n approximate
1	$(1/2)I(1)$	$(1/2)I(1)$
2	$(1/4)I(2)$	$(1/4)I(2)$
4	$-(1/8)I(4) \simeq -(1/8)6.00295$	$-(1/8)6$
6	$(1/4)I(6) \simeq (1/4)6.00005$	$(1/4)6$
8	$-(17/16)I(8) \simeq -(17/16)6.0$	$-(17/16)6$
10	$-(93/12)I(10) \simeq -(93.12)6.0$	$-(93/12)6$

Also shown in Figure 6 is $g(W)$ obtained by a numerical inversion of the characteristic function eq 3.4. Also here we use a finite system, however now we use a much larger system than $m = 8$. To find the numerical Fourier transform of the characteristic function we use an upper cutoff k_c, in such a way that $\langle \exp(ikW) \rangle = 0$, for $k > k_c$. The exact expression of $\langle \exp(ikW) \rangle$, for any finite system, is a periodic function of k, the period becoming very long as the size of the system is increased. Since we use the upper cutoff k_c in our numerical simulations we do not see the solution as a sum of closely spaced Δ peaks. Rather the approximate solution eq 5.2, the exact solution based on eq 3.5 and the numerical Fourier transform, all presented in Figure 6, are in good agreement.

A quantitative comparison between the exact and approximate solution is made using cumulants. The cumulants of the exact solution, eq 3.6, can be found in terms of the lattice sums $I(n)$. In Table 3 we give the exact cumulants (i.e., for $p = 1/2$) and the cumulants calculated based on the approximation eq 5.2 (notice that these results are not the conditional cumulants presented in Table 2). Using the results in Table 1, for the lattice sums $I(n)$, we see a good agreement between the exact and the approximate cumulants.

Our method used the conditional probabilities Prob ($W = x|n_1 = j_1$). One can generalize this approach by defining

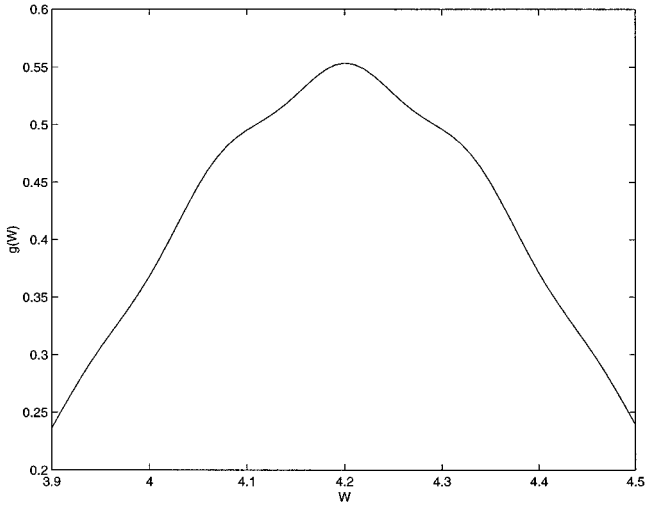

Figure 7. The central peak of $g(W)$ vs W for $p = 1/2$. We show the small secondary oscillations due to the next and next to next neighboring lattice points.

conditional probabilities for nearest neighbor, next-nearest neighbors, etc. In Figure 7 we show the output of such a computation. We have added the effect of next-nearest neighbors and next-to-next nearest neighbors to our calculation of $g(W)$. In this case $g(W)$ is a sum of $7 \times 13 \times 9$ Gaussians. In Figure 7 we show the central peak of $g(W)$ vs W. One can observe secondary small oscillations.

Finally, we note that for $p \simeq 1/2$ similar approximate solutions can be found using the same arguments as for the case $p = 1/2$. Then, one may consider instead of a sum of seven symmetrical Gaussian a sum of seven non symmetric functions (i.e., modified Gaussians). For $p \ll 1$, the situation is very different since then the inequalities eq 5.1 do not hold. This situation is discussed in section VII.

VI. Continuum Limit−Lévy Statistics

The continuum version of the model was investigated[8,9,11,28] in a context of a single molecule embedded in a glassy material. The model considers $N \rightarrow \infty$ uncorrelated TLSs, distributed uniformly in space and interacting with the molecule in the origin. Here we would like to point out the relation between this continuum model and Lévy stable distributions. In the following section we shall discus the relation between the continuum and lattice models in the limit $p \ll 1$.

The variance for the continuum model is

$$W = \sum_{i=1}^{N} x_i \geq 0 \tag{6.1}$$

and $x_i \equiv 1/r_i^6$. Equation 6.1 describes a random walk in which the length of each independent step is x_i. Therefore the central limit theorem and its generalization is of fundamental importance.[22−24] While the standard Gaussian central limit theorem applies when the variance of x_i converges, the generalized central limit theorem applies when the variance of x_i diverges. The problem at hand can be analyzed in terms of the generalized central limit theorem.

Let $\xi(x)$ be the probability density function describing $\{x_i\}$ which are independent identically distributed random variables. The probability density function $\xi(x)$ is related to the probability density of the random variables $\{r_i\}$, $\rho(r)$ according to $\xi(x) = |dr/dx|\rho(r)$. Using a uniform distribution of defects, $\rho(r)dr \sim r^2 dr$ we find

$$\xi(x) \sim x^{-(1+\gamma)} \tag{6.2}$$

and $\gamma = 1/2$, which means that the first moment of the summand x_i diverges. Hence, according to the generalized central limit theorem, the distribution of variance will be a non symmetrical (i.e., because $W \geq 0$) stable distribution with a characteristic exponent $\gamma = 1/2$. For this case the stable characteristic function is

$$\langle \exp(ikW) \rangle = \exp[-A|k|^{1/2}(1 - ik/|k|)] \tag{6.3}$$

and a short calculation shows $A \equiv p(2\pi)^{3/2}/3$ (here p is a dimensionless density). Equation 6.3 is one of the few stable characteristic functions which can be analytically inverted. The probability density of the variance is

$$g(W) = \frac{1}{A^2}\frac{2}{\sqrt{\pi}}\left(\frac{2W}{A^2}\right)^{-3/2}\exp\left(-\frac{A^2}{2W}\right) \tag{6.4}$$

also known as Smirnov's density.[30] In probability theory eq 6.4 describes the limit distribution of first return times of a one-dimensional Brownian motion. Similar to the probability density function $\xi(x) \sim x^{-3/2}$, the probability density function (6.4) decays as $g(W) \sim W^{-3/2}$.

We see that in the continuum limit the variance averaged over disorder diverges. This is because in the continuum model the TLSs are allowed to be situated very close to the molecule on the origin. A more physical approach would be to consider a lower cutoff (in the lattice model this is the lattice spacing). Then the distribution of variance would not be stable; however, for small enough cutoff one can still observe the characteristic $W^{-3/2}$ decay with an upper cutoff for large W (Pfluegl et al.[9] calculated the explicit dependence of the distribution of variance on the cutoff). Numerical simulations[10,11] and experiments[8] in glassy material show that the probability density of line widths $h(\Delta\nu)$, related to the probability density of variances according to eq 2.5, has a long tail; however, there is not sufficient data to determine if this distribution is related to Lévy statistics.

Very recently, Geva and Skinner,[11] on the basis of a continuum model similar to ours, showed that the probability density of moments of a frequency-frequency auto correlation function in low-temperature glasses all fit a universal master curve (eq 2.20 in ref 11). This master curve is Smirnov's density eq 6.4. This interesting result is also a consequence of the generalized central limit theorem.

VII. Continuum Approximation vs Lattice Model: $p \ll 1$

What is the relation between the solution of the continuum and lattice models? One might anticipate that for low defect density, $p \ll 1$, the TLSs situated far away from the molecule play an important role and then the lattice structure is of lesser importance. We rewrite the characteristic function eq 3.4 as

$$\langle \exp(ikW) \rangle_{\text{lat}} = \exp\{\sum_j \ln[1 + p(e^{ik/|j|^6} - 1)]\} \tag{7.1}$$

and the subscript indicates that we are considering a lattice model. We expand the logarithm to obtain

$$\langle \exp(ikW) \rangle_{\text{lat}} = \exp[-p\sum_j (1 - e^{ik/|j|^6})] \tag{7.2}$$

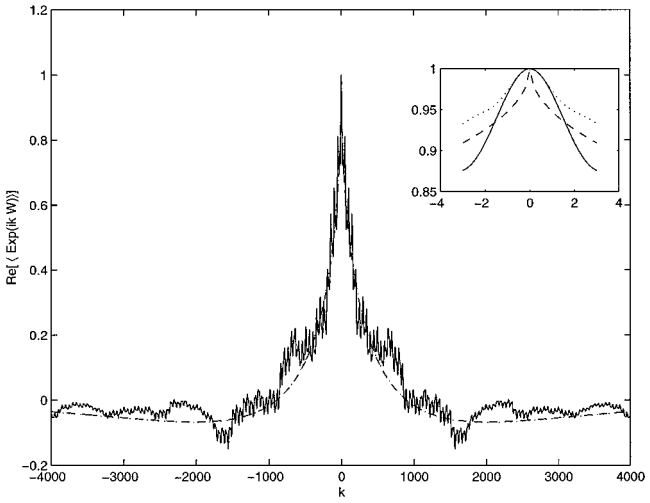

Figure 8. The real part of the characteristic function vs the Fourier variable k, with $p = 0.01$. The fluctuations of the exact lattice solution (solid curve) are due to the lattice structure and are not a finite size effect. The stable Smirnov characteristic function (dashed curve), with $A = p(2\pi)^{3/2}/3$, obtained from a continuum picture with no cutoff and a continuum characteristic function with a finite cutoff (dotted curve) are indistinguishable on the scale of the plot. In the inset we show the behavior of the exact and continuum solutions for small k. Notice the non analytical behavior of the stable characteristic function at $k = 0$. The exact lattice characteristic function as well as the continuum model exhibit an analytical behavior close to $k = 0$, due to the cutoffs a and r_c, respectively. We have chosen $r_c = [(4\pi p)/9\langle W^2\rangle_{lat}]^{1/9} = 0.838$, so that for values $k \ll 1$ the analytical continuum model and the lattice model exhibit similar behaviors.

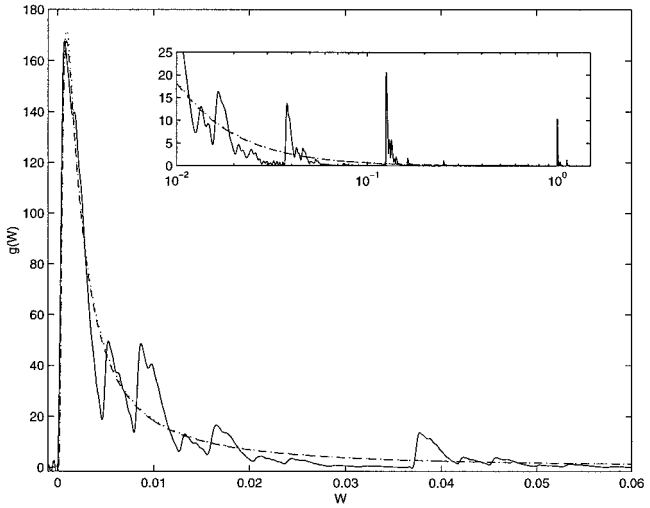

Figure 9. The solid curve is $g(W)$ for the case $p = 0.01$, obtained by a numerical Fourier transform of the lattice characteristic function. Dashed curve is Smirnov's stable probability density function obtained within the continuum approximation with $r_c = 0$. The deviations between the lattice and continuum model are large in the tail of the probability density function. Also shown is the continuum solution with a finite cutoff r_c (dotted curve), which on the scale of the plot is indistinguishable from the continuum model with no cutoff. In the inset we show the tail of $g(W)$ on a semilog plot.

for $p \ll 1$. The small k behavior of eq 7.2 is

$$\langle \exp(ikW)\rangle_{lat} \sim 1 + ipI(1)k - \frac{pI(2)}{2}k^2 + ... \qquad (7.3)$$

Converting the sum in eq 7.2 into an integral, we find

$$\langle \exp(ikW)\rangle_{con} = \exp[-p4\pi/3\int_{r_c}^{\infty} dr^3(1 - e^{ik/|r|^6})] \quad (7.4)$$

where r_c is a low cutoff and the subscript indicates that we are considering a continuum model. The continuum characteristic function eq 7.4 was analyzed in ref 9, integrating by parts

$$\langle \exp(ikW)\rangle_{com} = \exp\Big\{-\frac{4\pi}{3}pr_c^3\Big[\pi\sqrt{|y|}\Big[S(\sqrt{|y|}) - i\frac{y}{|y|}C(\sqrt{|y|})\Big] - (1 - e^{i\pi y/2})\Big]\Big\} \quad (7.5)$$

where $S(x)$ and $C(x)$ are the tabulated Fresnel sine and cosine integrals and $y \equiv (2l)/(\pi r_c^6)$.[31] Taking the limit $r_c \to 0$, in eq 7.5, we obtain the stable characteristic function eq 6.3. The small k behavior of the continuum characteristic function, eq 7.5 is

$$\langle \exp(ikW)\rangle_{com} \sim 1 + i\frac{4\pi}{3}\frac{p}{r_c^3}k - \frac{2\pi}{9}\frac{p}{r_c^9}k^2 \qquad (7.6)$$

where we have neglected terms proportional to p^2. Equation 7.6 exhibits an analytical behavior and therefore the moments of the continuum model with finite cutoff r_c converge; this is different from the nonanalytical behavior of the stable characteristic function eq 6.3 whose moments diverge.

In Figure 8 we use the exact solution of the lattice model eq 7.1 to show the real part of $\langle \exp(ikW)\rangle_{lat}$ as a function of k. Also shown in Figure 9 is Smirnov's stable characteristic function eq 6.3 together with the continuum model with a cutoff eq 7.5. The lattice solution exhibits large oscillations which look random. In contrast, the continuum solution with and without a cutoff behave smoothly. Choosing $r_c \simeq a = 1$, the continuum solutions with and without a cutoff are very much alike, except for small values of k. The exact lattice results were calculated for a finite system. We have checked that the solution does not depend on the size of the system.

In Figure 9 we show $g(W)$, obtained using numerical Fourier transform of the exact solution eq 7.1. We observe satellite peaks due to the lattice structure. These peaks are separated by large gaps in which $g(W) \simeq 0$. While $g(W)$ is mostly concentrated in a small region close to the origin (say $W < 0.01$), corresponding to interaction with distant defects, nevertheless, rare events with very large variance W are predicted to be significant.

Also shown in Figure 9 are the stable Smirnov density eq 6.4 and the numerical Fourier transform of the characteristic function with finite cutoff r_c eq 7.5. We find qualitative agreement between the lattice and continuum models, but only for small W. The deviation of the lattice solution from the continuum solution is most significant in the large W tail of $g(W)$ where the continuum models predicts a power law decay. This behavior can be easily understood. A molecule whose variance W is large implies that lattice points close to the origin are occupied by defects. For the defects close to the origin we can hardly expect a continuum model to work well. Since the continuum approximation does not work well we develop qualitative approximation valid for small p in the following subsection.

A. Weak Disorder Quantitative Approximation. The origin of the satellite peaks shown in Figure 10 is now investigated. We follow an approached sketched by Stoneham (see section 5.2 in ref 1) and used by Orth et al.[32] in the context of inhomogeneous line broadening. We divide the crystal into two regions. Within the first spherical inner region, which we call region 1, the lattice is treated as discrete and the rest of the crystal, region 2, is treated as a continuum. The radius of the

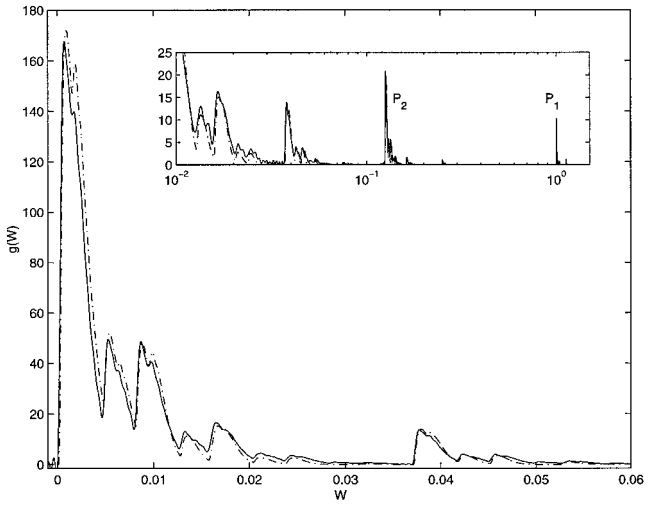

Figure 10. The same as Figure 9 with the approximate solution, eq 7.11 added. To obtain the approximate result we used $l = 9$.

inner region is $\sqrt{l}$ and l is an integer. We write

$$\text{Prob}\,(W = x) = \sum_{j_1,\ldots,j_l} Q_{j_1,\ldots,j_l}\text{Prob}\,(W = x|n_1 = j_1, \ldots, n_l = j_l) \tag{7.7}$$

with

$$Q_{j_1,\ldots,jl} = (1-p)^{N-\sum_{i=0}^{l} j_i} p^{\sum_{i=0}^{l} j_i} \binom{6}{j_1} \ldots \binom{n_l^{\max}}{j_l} \tag{7.8}$$

and $N = \sum_{i=1}^{l} n_i^{\max}$. Here Prob $(W = x|n_1 = j_1, \ldots, n_l = j_l)$ is the probability that $W = x$ subject to the condition that the number of n_1 sites is j_1, etc. The sum is over $j_1 = 0, \ldots, 6$, etc. Our approximation, valid for $p \ll 1$, involves two steps, first we replace the conditional probabilities Prob $(W = x|n_1 = j_1, \ldots, n_l = j_l)$ with smooth normalized nonnegative probability densities and then truncate the sum eq 7.7. The integer l in eq 7.7 divides the system into two, and the limit of large l must be considered. Practically, we increase l until our results converge. As in section V, we replace the discrete Prob $(W = x)$—with the continuum probability density function $g(W)$.

The first step is to replace the conditional probability Prob $(W = x|n_1 = j_1, \ldots, n_l = j_l)$, in eq 7.7, with its continuum approximation. For this aim we use the conditioned characteristic function

$$\langle \exp(ikW)\rangle_{n_1=j_1,\ldots,n_l=j_l} = e^{ikx_{\min}}\{\prod_{j\neq j_1,\ldots,j_l} [p\exp(ik/|j|^6) + (1-p)]\} \tag{7.9}$$

where the multiplication is over all lattice points excluding those in region 1 and with $x_{\min} = \sum_{i=1}^{l} j_i/i^3$. We now use the same procedure given in eqs 7.1—7.5, and then Prob $(W = x|n_1 = j_1, \ldots, n_l = j_l)$ in eq 7.7 is replaced with

$$g_{j_1,\ldots,j_l}(W) = \begin{cases} Sm(r_c, W - x_{\min}) & \text{if} \quad W > x_{\min} \\ 0 & \text{if} \quad W < x_{\min} \end{cases} \tag{7.10}$$

where $Sm(r_c, W)$ is the inverse Fourier transform of the continuum characteristic function eq 7.5. $Sm(r_c, W)$ is found here numerically. In eq 7.10 $r_c = \sqrt{l}$ is the low cutoff reflecting the fact that we are treating region 2 as a continuum. The main assumption that we are using is that when l is large enough the exact lattice sums may be replaces with the appropriate integrals.

For large l, the summation in eq 7.7 is formidable, for example, if $l = 9$, the sum is over e^{21} states. However, since $p \ll 1$ we may use a second approximation and truncate the sum in eq 7.7. The lowest order of approximation is to consider only the term proportional to $Q_{0,0,\ldots,0}$, and this term gives the contribution from an empty region 1. The first-order corrections are l terms in eq 7.7 proportional to $Q_{1,0,0,0,\ldots}$, $Q_{0,1,0,0,\ldots}$, etc. These terms imply that a single defect is residing in region 1. The $l(l+1)/2$ second-order terms are $Q_{1,1,0,0,\ldots}$, $Q_{1,1,0,0,\ldots}$, etc., and $Q_{2,0,\ldots}$, $Q_{0,2,\ldots}$, etc. We therefore find

$$g(W) = Q_{0,\ldots,0}g_{0,\ldots,0}(W) + \sum_{j_1+j_2+\ldots j_l=1} Q_{j_1,\ldots,j_l}g_{j_1,\ldots,j_l}(W) + \sum_{j_1+j_2+\ldots j_l=2} Q_{j_1,\ldots,j_l}g_{j_1,\ldots,j_l}(W) + \ldots \tag{7.11}$$

where the summation $\sum_{j_1+j_2+\ldots j_l=1}$ is over all values of $j_1 \geq 0$, $j_2 \geq 0$...which satisfy the condition $j_1 + j_2 + \ldots j_l = 1$.

The probability that region 1 is empty for a very large l and finite p is given by

$$Q_{0,0,0,\ldots} = \lim_{l\to\infty}(1-p)^N = 0 \tag{7.12}$$

and then the truncation procedure is not valid. Our approximation will work well only if l is large; however, p is small enough to ensure that the truncated sum eq 7.11 is approximately normalized to unity. For a given p and l this can be easily checked, since the functions $Sm(r_c, W - x_{\min})$ in eq 7.11 are normalized, probability densities.

Figure 10 shows the approximate solution eq 7.11 together with the results obtained using numerical Fourier transform of the characteristic function eq 7.1, for the case $p = 0.01$. The approximation was calculated using the first- and second-order correction terms. Good agreement between the numerical and approximate result is found. Each peak we observe in Figure 10 can be related to a microscopic configuration of defects within region 1. For example, the peaks labeled P_1 (P_2) in Figure 10 correspond to a defect situated on one of the nearest neighbor (next to nearest neighbors) sites, respectively. We notice that peak P_2 is taller than peak P_1; this is due to the fact that for a three-dimensional cubic lattice the number of next-nearest sites is larger than the number of nearest sites. Hence the probability that the "second shell" will be occupied is larger than the "first shell".

B. Gaussian and Lévy Behaviors. According to eq 6.3, a signature of stable behavior in k space is

$$Re[\log\langle \exp(ikW)\rangle_{\text{con}}] = -\frac{(2\pi)^{3/2}}{3}p|k|^{1/2} \tag{7.13}$$

On the other hand the exact small p behavior of the lattice model shows

$$Re[\log\langle \exp(ikW)\rangle_{\text{lat}}] = -p\sum_j \left[1 - \cos\left(\frac{k}{|j|^6}\right)\right] \tag{7.14}$$

The two-solution eq 7.13 and eq 7.14 are clearly different with the lattice solution exhibiting strong oscillations.

To use the continuum approximation for quantitative purposes one has to define statistical functions that are not sensitive to the lattice structure. One may filter out the lattice oscillations

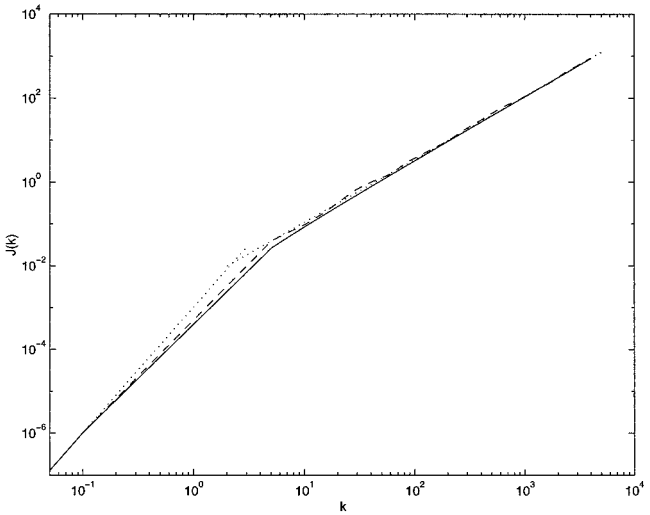

Figure 11. The case $p = 0.001$, $r_c = 0.847$. The dashed curve is the exact lattice result, the continuous curve is the continuum approximation, the dotted curves are the small k and large k asymptotic behaviors. We observe a crossover from Gaussian behavior for $k \ll 1$ and $J(k) \sim k^3$ to Lévy behavior with $J(k) \sim k^{3/2}$ for $k \gg 1$. The interesting feature is that only two distinct scaling regimes are seen.

by defining

$$J(k) \equiv -\int_0^k Re[\log\langle\exp(ik'W)\rangle]\mathrm{d}k' \qquad (7.15)$$

The small and large k behaviors of this function are

$$J_{lat}(k) = \begin{cases} \frac{p}{6} I(2)\, k^3 & k \ll 1 \\ \frac{2A}{3} k^{3/2} & k \gg 1 \end{cases} \qquad (7.16)$$

where A was defined in eq 6.3. The small k behavior can be understood on the basis of the integration of

$$Re[\log\langle\exp(ikW)\rangle_{lat}] \sim k^2 pI(2)/4 \qquad k \ll 1 \quad (7.17)$$

For larger k we get the stable behavior which can be predicted on the basis of

$$Re[\log\langle\exp(ikW)\rangle_{lat}] \sim -A|k|^{1/2} + \text{fluct} \qquad (7.18)$$

The fluctuation term in eq 7.18 becomes very small after an integration with respect to k (i.e., after filtering out the lattice oscillations). A more detailed calculation based on the continuum model eq 7.5 gives

$$J_{con}(k) = p\frac{4\pi}{9}\left\{2k^{3/2}\sqrt{2\pi S}\left(\sqrt{\frac{2k}{\pi r_c^6}}\right) + r_c^3[-3k + 2k\cos(k/r_c^6) + r_c^6 \sin(k/r_c^6)]\right\} \qquad (7.19)$$

Figure 11 presents $J(k)$ for the lattice model eq 7.1, for the continuum model eq 7.19, and for the asymptotic results eq 7.16. As can be seen, the continuum and lattice solutions are in good agreement. The reason for this is that we are considering the function $J(k)$ which does not depend strongly on the lattice structure. The main reason to consider such a function is that it exhibits two well-known behaviors. The first is an analytical small k Gaussian behavior which is controlled by the low lattice cutoff and the converging moments of the distribution function. The second $k^{3/2}$ behavior, for large k, can be traced back to the tails of the distribution and the stable characteristic function. The crossover between the two behaviors is controlled by the low cutoff (i.e., the lattice spacing in the lattice model).

VIII. Discussion

Stoneham[1] has used the so-called "statistical method" to analyze inhomogeneous line broadening. This approach uses a continuum approximation for the lattice structure and was used here to analyze the continuum model. We have used two other techniques to analyze the lattice model.

(a) We have found the exact solution of the lattice model eq 3.5. This solution exhibits many peaks, their number increasing sharply with the size of the system; hence, exact results can be obtained only for finite systems. Most applications are concerned with the infinite crystal limit for which only a smooth continuum solution is meaningful. Using a histogram, and for $p = {}^1/_2$, we were able to construct a smooth exact solution, for large enough systems, in such a way that the exact finite size solution agrees quantitatively with a solution obtained by numerically inverting the characteristic function.

(b) We use the mathematical theory of stable distributions (i.e., the generalized central limit theorem) to analyze the continuum model and show that $g(W)$ is Smirnov's stable density with index $\gamma = {}^1/_2$.

One may use the mathematical theory on stable distributions to generalize the continuum results with $r_c = 0$. Consider a generalized interaction with $W = \sum_j 1/|r_j|^\theta$ in dimension D. Then assuming a uniform density of defects, $g(W)$ will be a nonsymmetrical Lévy stable probability density with $\gamma = D/\theta \le 1$. For our model $D = 3$ and according to eq 2.3, $\theta = 6$ and hence $\gamma = {}^1/_2$. If we consider a two-dimensional system, with similar three-dimensional dipole interaction $\theta = 6$, we get $\gamma = {}^1/_3$. Then $g(W)$, given in closed form in ref 33, follows $g(W) \sim W^{-4/3}$, which is slower than the decay of $g(W)$ when $D = 3$. It is also interesting to point out that two symmetrical stable distributions are used to analyze inhomogeneous line broadening, these being Holtsmark line shape with $\gamma = {}^3/_2$, and the Lorentzian line shape $\gamma = 1$.[1] Furukawa, Nakai, and Kunitomi[34] have used Mössbauer spectroscopy and found that the distribution of internal magnetic fields in Au(Fe) spin glass alloys is Lévy stable. Zumofen and Klafter[18] have shown that the short time evolution of a single molecule coupled to a system of two levels systems is described by symmetrical Lévy stable Green functions. As mentioned in section VI, Geva and Skinner,[11] have shown that moments of a certain dynamical auto correlation function are also described by a stable distribution. All these results are a manifestation of the generalized central limit theorem[22-24] which was shown to play an important role in diverse physical phenomena.[35,36]

The generalized central limit theorem can be used when (a) the defects interact with the molecule according to a slow power law (b) the defects are distributed uniformly is space (i.e., with $r_c = 0$) (c) the defects are non interacting (d) the defects are statistically identical (e.g., all TLS-chromophore couplings are assumed identical). The relaxation of some of these assumptions was investigated in some detail. For example, the effect of introducing a cutoff[9] or interacting TLSs[16] or the inclusion of distributions of TLSs parameters[10] or lattice structure as considered here, all result in deviations from the Lévy stable behavior. However, under certain conditions these deviations may become small and then the stable behavior may be expected to hold.

The slow power law decay of $g(W)$ found within the continuum picture is a result of defects situated close to the molecule. In the lattice results and for p=0.01, this power law

is not found; rather, we observe well separated peaks in the tail of $g(W)$. Hence the large W behavior of $g(W)$ is very sensitive to the lattice structure. This is expected, since defects in the vicinity of the molecule contribute to the large W behavior of $g(W)$ and then the lattice structure cannot be approximated by a continuum.

It is interesting to note that lattice models of inhomogeneous line broadening by point defects predict the appearance of satellite structure in the inhomogeneous line shape.[1,32] Such satellite structure was observed experimentally and was claimed[1,32] (and references therein) to reflect the lattice structure. The satellite structure reported in[32] is rather weak, suggesting that the lattice structure is only slightly perturbing the inhomogeneous line shape of the appropriate continuum model. On the other hand, as we show here, the distribution of variance $g(W)$ exhibits a strong sensitivity to the lattice structure. As observed in Figures 6 and 10 the lattice structure is not a weak perturbation, slightly modifying continuum results, but rather has a strong influence on the density of variances $g(W)$. The reason for this is that the effective interaction exponent in eq 2.3 is 6; hence, the interaction decays in space rather fast and this in turn implies a strong sensitivity on the occupation of nearby neighbors and hence on the structure of the lattice.

In glassy materials our results are clearly not quantitatively valid. In calculations[8,9,11,28] of the distribution of variances it has been assumed that the glass has no structure and that the defects two level systems are distributed uniformly in space. This assumption is valid for large distances from the chromophore. We believe that the short range structure of the glass may influence the distribution of line widths. This is expected to be observed mainly in the tail of the distribution.

Reilly and Skinner[37] have modeled spectral diffusion of pentacene in p terphenyl crystal,[7] using what they have called a 2D model. They associate TLSs with lattice sites in a plane at a given distance from the single molecule. This modeling is motivated by the assumption that the dominant contribution to spectral diffusion arises from TLSs residing on domain walls. These domains are characterized by TLSs with different orientation. The Skinner Reilly model is different than ours since we assume that the occupation probability of each lattice site is independent of the occupation of other sites.

In this work we have assumed that the molecule in the origin does not distort the lattice structure. When the size of the molecule is approximately identical to the size of the host molecule, this assumption is reasonable. The variance might be controlled by mechanisms different than ours for example due to coupling to phonon bath, laser intensity, and detection efficiency,[38] we have assumed that all these effects are negligible. Other assumptions we have used are discussed in Section II.

Acknowledgment. The research was supported in part by a grant from the NSF Chemistry division. E.B. thanks Younjoon Jung for helpful discussion.

IX. Appendix A

To construct the solution we rewrite the characteristic function for a finite system

$$\langle \exp(ikW)\rangle = [\mathrm{p}e^{ik} + (1-p)]^{n_1^{\max}}[\mathrm{p}e^{ik/2^3} + (1-p)]^{n_2^{\max}}[\mathrm{p}e^{ik/3^3} + (1-p)]^{n_3^{\max}}\ldots[\mathrm{p}e^{ik/m^3} + (1-p)]^{n_m^{\max}} \quad (9.1)$$

where m is an upper cutoff and we want to consider the limit of large m. Using the Binomial expansion

$$\langle \exp(ikW)\rangle = \left[\sum_{n_1=0}^{n_1^{\max}} \binom{n_1^{\max}}{n_1} (py)^{n_1}(1-p)^{n_1^{\max}-n_1}\right] \times \left[\sum_{n_2=0}^{n_2^{\max}} \binom{n_2^{\max}}{n_2} (py^{1/2^3})^{n_2}(1-p)^{n_2^{\max}-n_2}\right]\ldots \left[\sum_{n_m=0}^{n_m^{\max}} \binom{n_m^{\max}}{n_m} (py^{1/m^3})^{n_2}(1-p)^{n_m^{\max}-n_{\mathrm{m}}}\right] \quad (9.2)$$

with $y = \mathrm{e}^{ik}$ and rearranging the summations we find

$$\langle \exp(ikW)\rangle = \sum_{n_1}^{n_1^{\max}}\sum_{n_2}^{n_2^{\max}}\ldots\sum_{n_m}^{n_m^{\max}} \binom{n_1^{\max}}{n_1}\binom{n_2^{\max}}{n_2}\ldots \binom{n_2^{\max}}{n_2} p^{\sum_{i=1}^{m} n_i}(1-p)^{N-\sum_{i=1}^{m} n_i} y^{n_1+n_2/2^3+\ldots n_m/m^3} \quad (9.3)$$

where $N = \sum_{i=1}^{m} n_i^{\max}$ is the number of lattice sites. We use the inverse Fourier transform to find eq 3.5.

References and Notes

(1) Stoneham, A. M. *Rev. Mod. Phys.* **1969**, *41*, 82.
(2) Bache, T., Moerner, W. E., Orrit, M., and Wild, U. P., Eds. *Single-Molecule Optical Detection, Imaging and Spectroscopy*; VCH: New York, 1996.
(3) Nie, S.; Zare, R. N. *Annu. Rev. Biophys. Biomol. Struct* **1997**, *26*, 567.
(4) Plathotnik, T.; Donley, E.; Wild, Urs P. *Ann. Rev. Phys. Chem.* **1997**, *48*, 181.
(5) Xie, X. S.; Trautman, J. K. *Ann. Rev. Phys. Chem.* **1998**, *49*, 441.
(6) Moerner, W. E.; Orrit, M. *Science* **1999**, *283*, 5408.
(7) Ambrose, W. P.; Bache, T.; Moerner, W. E. *J. Chem. Phys.* **1991**, *95*, 7150.
(8) Fleury, L.; Zumbusch, A.; Orrit, M.; Brown, R.; Bernard, J. *J. Lumin.* **1993**, *56*, 15.
(9) Pfluegl, W.; Brown, F. L. H.; Silbey, R. J. *J. Chem. Phys.* **1998**, *108*, 6876.
(10) Geva, E.; Skinner, J. L. *J. Phys. Chem. B* **1997**, *101*, 8920.
(11) Geva, E.; Skinner, J. L. *Chem. Phys. Lett.* **1998**, *287*, 125.
(12) Suarez, A.; Silbey, R. *Chem. Phys. Lett.* **1994**, *218*, 445.
(13) Suarez, A.; Silbey, R. *J. Phys. Chem.* **1994**, *98*, 7329.
(14) Reilly, P. D.; Skinner, J. L. *J. Chem. Phys.* **1994**, *101*, 959.
(15) Reilly, P. D.; Skinner, J. L. *J. Chem. Phys.* **1998**, *108*, 7434.
(16) Brown, F. L. H.; Silbey, R. J. *J. Chem. Phys.* **1998**, *108*, 7434.
(17) Narasimhan, L.; Littau, K.; Pack, D.; Bai, Y.; Elschner, A.; Fayer, M. *Chem. Rev.* **1990**, *90*, 439.
(18) Zumofen, G.; Klafter, J. *Chem. Phys. Lett.* **1994**, *219*, 303.
(19) Tanimura, Y.; Takano, H.; Klafter, J. *J. Chem. Phys.* **1998**, *108*, 1851.
(20) Zhao, Y.; Chernyak, V.; Mukamel, S. *J. Phys. Chem. A* **1998**, *102*, 6614.
(21) Barkai, E.; Silbey, R. *Chem. Phys. Lett.* **1999**, *310*, 287.
(22) Lévy, P. *Théorie de l'addition des variables aléatories*; Gauthier-Villars: Paris, 1937.
(23) Gnedenko, B. V.; Kolmogorov, A. N. *Limit Distributions for Sums of Independent Random Variables*; Addison-Wesley: Reading, MA, 1954.
(24) Feller, W. *An Introduction to Probability Theory and Its Applications*; John Wiley and Sons, New York; 1970, Vol. 2.
(25) Tittel, J.; Kettner, R.; Basche, Th.; Brauchle, C.; Quante, H.; Mullen, K. *J. Lumin.* **1995**, *64*, 1.
(26) Vacha, M.; Liv, Y.; Nakatsuka, H., Tani, T. *J. Chem. Phys.* **1997**, *106*, 8324.
(27) Kozankiewicz, B.; Bernard, J.; Orrit, M. J. *J. Chem. Phys.* **1994**, *101*, 9377.
(28) Fleury, L., Ph.D. Thesis, University of Bordeaux, Brodeaux, France, 1995.
(29) The continuum approximation works well only when a lower cutoff is introduced in the appropriate integral. For distances shorter than this cutoff the lattice must be treated as discrete.

(30) Montroll, E. W.; West, B. J. In *Fluctuation Phenomena*; Montroll, E. W., Lebowitz, J. L., Eds.; North Holland: Amsterdam, 1987.

(31) Abramovitz, M.; Stegun, I. A. *Handbook of Mathematical Functions*; Dover Publications, Inc.: New York, 1970.

(32) Orth, D. L.; Mashl, R. J.; Skinner, J. L. *J. Phys.: Condens. Matter* **1993**, *5*, 2533.

(33) Montroll, E. W.; Bendler, J. T. *J. Stat. Phys.* **1984**, *34*, 129.

(34) Furukawa, Y. Nakai; Kunitomi, N. *J. Phys. Soc. Jpn.* **1993**, *62*, 306.

(35) Mandelbrot, B. *The Fractal Geometry of Nature*; Freeman: San Francisco, 1982.

(36) Klafter, J.; Shlesinger, M. F.; Zumofen, G. *Phys. Today* **1996**, *49*, 33.

(37) Reilly, P. D.; Skinner, J. L. *Phys. Rev. Lett.* **1993**, *71*, 4257.

(38) Kador, L. *J. Phys. Chem. A* **1998**, *102*, 9745.